International Journal of Engineering & Applied Sciences (IJEAS)
Vol.15, Issue 1 (2023) 19-35
http://dx.doi.org/10.24107/ijeas.1204338
Int J Eng Appl Sci 15(1) (2023) 19-35

The Effects of Calibration Parameters in Muskingum Models on Flood Prediction Accuracy

Olusegun O. Alabi [1], Abigail T. Olaoluwa [2], Samuel O. Sedara [3]*

[1,2]Department of Physics Osun State University, Osogbo, Nigeria
[3]Department of Physics and Electronics, Adekunle Ajasin University, Akungba-Akoko,Ondo State, Nigeria
[*]E-mail address: olusegun.alabi@uniosun.edu.ng[*], abigail.olaoluwa@uniosun.edu.ng , samuel.sedara@aaua.edu.ng

ORCID numbers of authors:
0000-0001-9088-8004[*], 0000-0001-8777-1702, 0000-0002-2116-1263

Received date: 15.11.2022
Accepted date:27.04.2023

Abstract

Attenuation, time lag, outflow peak and storage are very essential factors required in flood risk prediction and flood pattern. However, the accurate prediction strongly depends on appropriate calibration of routine parameters of the model, such as weighting factor (x) and storage time constant (K). The weighting factor being used to determine storage time constant has not been given consideration in the previous studies and this could have led to inaccurate prediction in the past. In this work, a set of data obtained from an ungauged Awara river in Ondo State, Nigeria were used to test the effects of a weighting factor, x at levels ranging from 0.1-0.5 at interval of 0.1. The Muskingum model was used to obtain the storage and weighted discharge storage. It was observed that the correlation coefficient (R^2) decreases with an increase in the weighting factor (x). This implies that there is a strong relationship between storage and weighted discharge storage at 0.1-0.3 levels of x while, the relationship is fair at 0.4-0.5 levels. It is therefore appropriate to choose a value of x ranging between 0.1 and 0.3 for attenuation prediction, while values of x ranging between 0.4 and 0.5 would be appropriate for accurate prediction of both outflow peak and storage.

Keywords: Muskingum model, Awara river, hydrograph, flood risk, Attenuation, outflow peak.

1. Introduction

Flooding occurs when an area is submerged in water. It is an overspill of large amount of water to a dry land which can be caused by over spilling from rivers, streams and even excessive rainfall [1-4]. The aftermath of floods is mostly associated with destruction of properties and loss of lives [5] because it can cart away bridges, cars, houses, and even humans and also destroys crops and trees on land [6].

Flooding occurs globally and causes casualties and property loss. It is undoubtedly the most overwhelming and common natural disaster in the human world [7]. It is also reported to be the most significant proportionate number of natural disasters happening globally and over the last four decades this percentage has increased and this led to significant research towards the development of flood inundation models [8]. Flooding can occur without any prior warnings and can cause many deaths and destruction of properties if the public is not warned in advance. The

public needs to be warned in an informative and timely manner to minimize the impacts of flood. This process involves the recognition of prediction commencement, gathering and assessment of data by computerized systems, threat recognition, notification, decision generation, response activation, and public action and mitigation strategies [9].
Most flood models involve background responsiveness and research to the productivity variables for predictive application in space and time scales. The level of precision required and computational efficiency is of utmost concern [10, 11]. Calibration of Parameters in flood forecasting is very important because there is challenge of getting discharge data for model calibration for flood prediction in ungauged basin or river. Therefore, rainfall runoffs are used for model calibration in ungauged basin or river. The reliability of runoff prediction in flood forecasting depends on proper calibration of model and this calibration parameters in Muskingum models are weighting factor *(x)* and storage time constant *(K)* [12, 13].
Many researchers have made use of Muskingum model to predict flood risks, ranges from agriculture, environment, dams, bridges construction and irrigation [14-17].

Ref. [18] used Adaptive Hydraulics (AdH) model and the Finite Element Surface Water Modeling System (FESWMS) to generate a hydraulic model in the Akarcay Basin area of Turkey. They first determined the peak flood discharges consisting of three methods and observed monthly flow data (hydrographs) from gauging stations and then used Synthetic methods, SCS & Mockus, to estimate peak flood discharges and finally the rainfall-runoff relationship was considered by using the observed monthly total precipitation data. Their results showed that the AdH and FESWMS models provided good results in shallow water modeling as in the case of Akarcay Basin rivers. Also [19] analysed vulnerability of flooding among Tharu households in Nepal using data collected from household surveys, group discussions, and key informant interviews in the Thapapur Village in the Kailali district, western Tarai, Nepal. Their theory was based on pressure and release (PAR) and access models. They finalized that the Tharu people are the major residents in the study area and they preferred to live within their community and also some marginalized people selected the location for residence. They also observed that human causalities have been reduced due to easy access to cell phones which has eased effective flood warnings with suitable lead times, but agriculture production loss and other losses are still high. Lastly they concluded that subsistence agriculture-based households with small land holding sizes and less income variation are highly susceptible to flooding.
However, the effect of calibration parameters range such as x and K have not been given consideration. The chosen value of x ranges between 0 and 0.5 and some researchers choose the calibration value without necessarily considering the significant of this value on their prediction accuracy. This work therefore examined the significance of calibration parameters in Muskingum model on flood prediction accuracy and determined the effects of calibration parameters; x and K on flood risk prediction accuracy in non-linear Muskingum model. This was achieved by investigating the ways in which calibration parameters can enhance the accuracy of flood risk prediction using hydrograph procedures. In addition, the hydrograph was obtained at different calibration parameter level of weighting factor and determining the effect of variation in calibration parameter weighting factor on flood prediction.

1.1 Theoretical Background

1.1.1 Flood routing

Flood routing is a procedure applied for prediction of variations in the shape and contour of a hydrograph as water passes through a river route or a reservoir [20]. There are two types of routing which are Reservoir and Channel routing. Reservoir routing is the study of effect of flood wave entering a reservoir. While, Channel Routing is the change in the shape of a hydrograph as it travels down a channel [21]. There are two types of flood modelling namely Hydraulic and Hydrologic are routing. Hydraulic routing is the hydraulic model that involves the collecting of data related to river geometry and these data are modelled and solved numerically. On the other hand the hydrologic routing applies the continuity equation for hydrology. In simple form the inflow to the river extent is equal to the outflow of the river extent plus the change of storage. The linear and nonlinear Muskingum models which are hydrologic models are essential to estimate hydrologic parameters using recorded data in both upstream and downstream part of rivers [22, 23].

1.1.2 Muskingum models for river flood routing

The established Muskingum model with the linear storage equation was developed for a district in Ohio for the control of flood in the 1930s (Muskingum conservancy district) [23]. Hydrological method for river routing is more complex than the reservoir routing because water storage in a reach is dependent on both inflow and outflow while in the reservoir routing case, the storage is generally dependent only on the outflow from the reservoir. The Muskingum Equation is:

$$\frac{ds}{dt} = I - Q \tag{1}$$

$$S = K[xI + (1 - x)Q] \tag{2}$$

Where S = Total Storage, K = Storage-time constant, x = Weighting factor takes value between 0 to 0.5, I = Inflow discharge, Q = Outflow discharge.
In this study, the common Muskingum equation as introduced below is used for flood routing computations:

$$O_2 = C_0 I_2 + C_1 I_1 + C_2 O_1 \tag{3}$$

In which,

$$C_0 = \frac{(-kx + 0.5\Delta t)}{k - kx + 0.5\Delta t} \tag{4}$$

$$C_1 = \frac{(kx + 0.5\Delta t)}{k - kx + 0.5\Delta t} \tag{5}$$

$$C_2 = \frac{k - kx - 0.5\Delta t}{k - kx + 0.5\Delta t} \tag{6}$$

C_0, C_1 and C_2 are coefficients of routing defined in terms of t, K and x as above.

I_1 = Inflow discharge at time t, I_2 = Inflow discharge at time $t+\Delta t$, O_1 = Outflow discharge at time t, O_2 = Outflow discharge at time $t+\Delta t$, Δt = time interval, K and x are the storage-time constant and weighting factor parameters which should be estimated through the calibration process [24]. K and x are the parameters to be determined from observations which have a value reasonably close to the flow travel time through the river reach, and x usually ranging between 0 and 0.5. Therefore, the key objective of the Muskingum model is to estimate the parameters K and x [25]. It is noted that the friction slope varies inversely with the area of the flow so that the value of the parameter x will be less than 0.5. The result has a value of x greater than 0.5, which would indicate amplification at all frequencies.

2. Materials and Methods

The data used for this work was gotten from [14, 15, 26] which was from a report of a dam located in Ondo North senatorial district. The procedure for routine started with the hydrologic parameters weighting factor *(x)* of 0.1 and time interval *(Δt)* of 30 days. The storage was calculated using the inflow and outflow data with the time interval where the initial outflows is equal to the initial inflows when the flood has not arrived. Then estimate the next storage for individual weighting factor *(x)* using the formula: $S = K[xI + (1-x)Q]$.
Thereafter, a plot of a chosen weighting factor (x) against the calculated was obtained to get storage-time constant *(k)*. Then the values of C_0, C_1 and C_2 were calculated from Eqs. (4-6). Later the new outflow was calculated using equation (3) and the plot of the graph of the inflow peak with the new calculated outflow *(Q)*. The above steps were repeated for other set of values of weighting factor *(x)* at interval of 0.1. The process for the work flow for this work is shown in Figure 1.

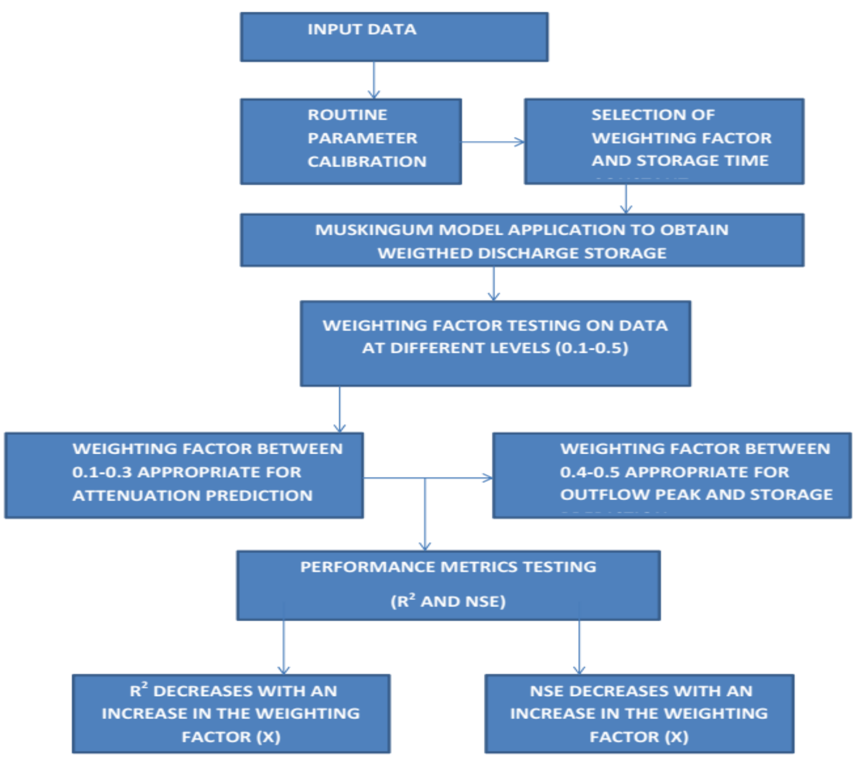

Fig. 1. Flow chart for the methodology for this work

3. Results and Discussion

The raw data extracted from detailed project reports from [26] is presented in Table 1 and the results of inflow and calculate storage with weighting factor (x) at 0.1, 0.2, 0.3, 0.4, and 0.5 respectively using equation 13 with Maple 2020 is presented in table 2 and was obtained in stepwise order; Columns 1-3 were gotten from the raw data obtained from detailed project report from [26]. Column 4: subtract column 3 from column 2 to obtain (I – O). Column 5: average of column 3 (adding two cells in column 3 divide it by 2) to obtain Avg (I – O). Column 6 is the multiplication of column 5 by 30days (change in time) to obtain ΔS=Col. 5xΔt and column 7 is the addition of first cell in column 7 that is 0 to the first cell in column 6 to obtain $S=\sum \Delta S$. Column 8-12 is computed using the equation 13 with x at 0.1, 0.2, 0.3, 0.4 and 0.5.
Tables 3,4,5,6 and 7 shows the calculated outflow at x = 0.1, 0.2, 0.3, 0.4, and 0.5. Column 1 is the time in days when the inflow was recorded with the interval of 30days for 12 months. Column 2 is the inflow rate in m^3/s per time interval. Column 3 is the product of routing coefficient C_0 and Inflow rate I_2. Column 3 is the product of routing coefficient C_1 and initial inflow rate I_1. Column 4 is the product of routing coefficient C_2 and initial outflow rate O_1. Column 5 is the addition of columns 3, 4, and 5 to give the calculated outflow Q in m^3/s.

Table 1. Raw data from Awara Dam/Oyimo River

Time (days)	Inflow (m^3/s)	Outflow (m^3/s)
0	0.01	0.01
30	0.002	0.009
60	0.064	0.014
90	0.979	0.156
120	0.105	0.4
150	0.129	0.275
180	0.149	0.214
210	0.131	0.183
240	0.161	0.164
270	0.128	0.159
300	0.035	0.134
330	0.067	0.096
360	0	0.074

Table 2. Comprehensive table showing the calculated storage.

Time (days)	**Inflow (m3/s)**	**Outflow (m3/s)**	**(I -O)**	**Avg(I -O)**	**ΔS=Col. 5xΔt**	**S=∑ΔS**	$[xI + (1-x)Q]$ (m^3/s)				
					m3/s.day	m3/s.day	*x=0.1*	*x=0.2*	*x=0.3*	*x=0.4*	*x=0.5*
0	0.01	0.01	0			0.000	0.01	0.01	0.01	0.01	0.01
30	0.002	0.009	-0.007	-0.0035	-0.105	-0.105	0.0083	0.0076	0.0069	0.0062	0.0055
60	0.064	0.014	0.05	0.0215	0.645	0.540	0.019	0.024	0.029	0.034	0.039
90	0.979	0.156	0.823	0.4365	13.095	13.635	0.2383	0.3206	0.4029	0.4852	0.5675
120	0.105	0.4	-0.295	0.264	7.92	21.555	0.3705	0.341	0.3115	0.282	0.2525
150	0.129	0.275	-0.146	-0.2205	-6.615	14.940	0.2604	0.2458	0.2312	0.2166	0.202
180	0.149	0.214	-0.065	-0.1055	-3.165	11.775	0.2075	0.201	0.1945	0.188	0.1815
210	0.131	0.183	-0.052	-0.0585	-1.755	10.020	0.1778	0.1726	0.1674	0.1622	0.157
240	0.161	0.164	-0.003	-0.0275	-0.825	9.195	0.1637	0.1634	0.1631	0.1628	0.1625
270	0.128	0.159	-0.031	-0.017	-0.51	8.685	0.1559	0.1528	0.1497	0.1466	0.1435
300	0.035	0.134	-0.099	-0.065	-1.95	6.735	0.1241	0.1142	0.1043	0.0944	0.0845
330	0.067	0.096	-0.029	-0.064	-1.92	4.815	0.0931	0.0902	0.0873	0.0844	0.0815
360	0	0.074	-0.074	-0.0515	-1.545	3.270	0.0666	0.0592	0.0518	0.0444	0.037

Table 3. Inflow and Calculated outflow data with $x = 0.1$

Time (days)	Inflow (m^3/s)	C_oI_2	C_1I_1	C_2O_1	Q (m^3/s)
0	0.01	0			0.010
30	0.002	0.0003	0.0030	0.0056	0.009
60	0.064	0.0084	0.0006	0.0051	0.014
90	0.979	0.1281	0.0195	0.0079	0.155
120	0.105	0.0137	0.2983	0.0878	0.400
150	0.129	0.0169	0.0320	0.2257	0.275
180	0.149	0.0195	0.0393	0.1550	0.214
210	0.131	0.0171	0.0454	0.1207	0.183
240	0.161	0.0211	0.0399	0.1034	0.164
270	0.128	0.0167	0.0491	0.0928	0.159
300	0.035	0.0046	0.0390	0.0895	0.133
330	0.067	0.0088	0.0107	0.0751	0.095
360	0	0.0000	0.0204	0.0534	0.074

Table 4. Inflow and Calculated outflow data with $x = 0.2$

Time (days)	Inflow (m^3/s)	C_oI_2	C_1I_1	C_2O_1	Q (m^3/s)
0	0.01	0			0.01
30	0.002	0.0001	0.0044	0.0050	0.0095
60	0.064	0.0038	0.0009	0.0048	0.0095
90	0.979	0.0584	0.0279	0.0048	0.0911
120	0.105	0.0063	0.4266	0.0460	0.4789
150	0.129	0.0077	0.0458	0.2416	0.2951
180	0.149	0.0089	0.0562	0.1489	0.2140
210	0.131	0.0078	0.0649	0.1079	0.1807
240	0.161	0.0096	0.0571	0.0912	0.1579
270	0.128	0.0076	0.0702	0.0796	0.1574
300	0.035	0.0021	0.0558	0.0794	0.1373
330	0.067	0.0040	0.0153	0.0693	0.0885
360	0	0.0000	0.0292	0.0447	0.0739

Table 5. Inflow and Calculated outflow data with $x = 0.3$

Time (days)	**Inflow (m^3/s)**	**C_0I_2**	**C_1I_1**	**C_2O_1**	**Q(m^3/s)**
0	0.01	0.0000			0.0100
30	0.002	0.0000	0.0060	0.0039	0.0100
60	0.064	0.0004	0.0012	0.0039	0.0055
90	0.979	0.0058	0.0385	0.0021	0.0465
120	0.105	0.0006	0.5897	0.0182	0.6085
150	0.129	0.0008	0.0632	0.2384	0.3024
180	0.149	0.0009	0.0777	0.1185	0.1971
210	0.131	0.0008	0.0897	0.0772	0.1677
240	0.161	0.0009	0.0789	0.0657	0.1456
270	0.128	0.0008	0.0970	0.0570	0.1548
300	0.035	0.0002	0.0771	0.0606	0.1379
330	0.067	0.0004	0.0211	0.0540	0.0755
360	0	0.0000	0.0404	0.0296	0.0699

Table 6. Inflow and Calculated outflow data with $x = 0.4$

Time (days)	**Inflow (m^3/s)**	**C_0I_2**	**C_1I_1**	**C_2O_1**	**Q (m^3/s)**
0	0.01	0.0000			0.01
30	0.002	0.0000	0.0080	0.0023	0.0102
60	0.064	-0.0014	0.0016	0.0023	0.0025
90	0.979	-0.0216	0.0509	0.0006	0.0298
120	0.105	-0.0023	0.7789	0.0068	0.7833
150	0.129	-0.0029	0.0835	0.1775	0.2582
180	0.149	-0.0033	0.1026	0.0585	0.1578
210	0.131	-0.0029	0.1185	0.0358	0.1514
240	0.161	-0.0036	0.1042	0.0343	0.1350
270	0.128	-0.0028	0.1281	0.0306	0.1558
300	0.035	-0.0008	0.1018	0.0353	0.1364
330	0.067	-0.0015	0.0278	0.0309	0.0573
360	0	0.0000	0.0533	0.0130	0.0663

Table 7. Inflow and Calculated outflow data with *x = 0.5*

Time (days)	Inflow (m^3/s)	C_0I_2	C_1I_1	C_2O_1	Q (m^3/s)
0	0.01	0			0.01
30	0.002	0.0000	0.0100	0.0002	0.0102
60	0.064	-0.0012	0.0020	0.0002	0.0010
90	0.979	-0.0186	0.0640	0.0000	0.0454
120	0.105	-0.0020	0.9790	0.0009	0.9779
150	0.129	-0.0025	0.1050	0.0186	0.1211
180	0.149	-0.0028	0.1290	0.0023	0.1285
210	0.131	-0.0025	0.1490	0.0024	0.1490
240	0.161	-0.0031	0.1310	0.0028	0.1308
270	0.128	-0.0024	0.1610	0.0025	0.1611
300	0.035	-0.0007	0.1280	0.0031	0.1304
330	0.067	-0.0013	0.0350	0.0025	0.0362
360	0	0.0000	0.0670	0.0007	0.0677

3.1. Computation of coefficients of routing

C_0, C_1 and C_2 are coefficients of routing defined in terms of *t, K and x* as above i.e:

$$C_0 = \frac{(-kx + 0.5\Delta t)}{k - kx + 0.5\Delta t}$$

$$C_1 = \frac{(kx + 0.5\Delta t)}{k - kx + 0.5\Delta t}$$

$$C_2 = \frac{k - kx - 0.5\Delta t}{k - kx + 0.5\Delta t}$$

For *x = 0.1 and k = 59.873,* $\Delta t = 30$days, then;

$$C_0 = \frac{(-59.873\times 0.1+0.5\times 30)}{59.873-59.873\times 0.1+0.5\times 30}; C_0 = 0.1308$$

$$C_1 = \frac{(59.873\times 0.1+0.5\times 30)}{59.873-59.873\times 0.1+0.5\times 30}; C_1 = 0.3047$$

$$C_2 = \frac{59.873-59.873\times 0.1-0.5\times 30}{59.873-59.873\times 0.1+0.5\times 30}; C_2 = 0.5645$$

For x = 0.2 and k = 56.933, $\Delta t = 30 days$

$$C_0 = \frac{(-56.933\times 0.2+0.5\times 30)}{56.933-56.933\times 0.2+0.5\times 30}; C_0 = 0.0597$$

$$C_1 = \frac{(56.933\times0.2+0.5\times30)}{56.933-56.933\times0.2+0.5\times30};\ C_1 = 0.4358$$

$$C_2 = \frac{56.933-56.933\times0.2-0.5\times30}{56.933-56.933\times0.2+0.5\times30};\ C_2 = 0.5045$$

For x = 0.3 and k = 49.037, $\Delta t = 30days$

$$C_0 = \frac{(-49.037\ \times0.3+0.5\times30)}{49.037\ -49.037\ \times0.3+0.5\times30};\ C_0 = 0.0059$$

$$C_1 = \frac{(49.037\times0.3+0.5\times30)}{49.037-49.037\ \times0.3+0.5\times30};\ C_1 = 0.6023$$

$$C_2 = \frac{49.037-49.037\times0.3-0.5\times30}{49.037\ -49.037\ \times0.3+0.5\times30};\ C_2 = 0.3918$$

For x = 0.4 and k = 39.646 $\Delta t = 30days$

$$C_0 = \frac{(-39.646\times0.4+0.5\times30)}{39.646-39.646\times0.4+0.5\times30};\ C_0 = 0.0221$$

$$C_1 = \frac{(39.646\times0.4+0.5\times30)}{39.646-39.646\times0.4+0.5\times30};\ C_1 = 0.7956$$

$$C_2 = \frac{39.646-39.646\times0.4-0.5\times30}{39.646\ -39.646\ \times0.4+0.5\times30};\ C_2 = 0.2266$$

For x = 0.5 and k = 31.161 $\Delta t = 30days$

$$C_0 = \frac{(-31.161\times0.5+0.5\times30)}{31.16-31.161\times0.5+0.5\times30};\ C_0 = -0.0190$$

$$C_1 = \frac{(31.161\times0.5+0.5\times30)}{31.161-31.16\times0.5+0.5\times30};\ C_1 = 1$$

$$C_2 = \frac{31.161-31.161\times0.5-0.5\times30}{31.161\ -31.161\ \times0.5+0.5\times30};\ C_2 = 0.0190$$

Figure (2) shows the plots of storage against weighted discharge storage for each level of weighting factor (x) used in this work. The storage time constant (k) was obtained from the equation of the plot for each level. It was observed that x varies inversely proportional to storage constant K because K decreases with an increase in x. Figure 2(a) has the equation of $59.873x + 0.647$ with a correlation coefficient, R^2 = 0.9999. Thus, parameter K is 59.873. Figure 2b has equation of $56.933x + 0.2499$ with a correlation coefficient, R^2 = 0.9451. Thus, parameter K is56.933. Figure 2(c) has equation of $49.037x + 0.8784$ with a correlation coefficient, R^2 = 0.8091. Thus, parameter K is 49.037. Figure 2(d) has equation of $39.646x + 2.2358$ with a correlation coefficient, R^2 = 0.6502. Thus, parameter K is 39.646. Figure 2(e) has equation of $31.161x + 3.4697$ with a correlation coefficient, R^2 = 0.5079. Thus, parameter K is 31.161. It was observed that correlation coefficient (R^2) decreases with an increase in the weighting factor (x). The correlation coefficients (R^2) are 0.9999, 0.9451, 0.8091, 0.6502, and 0.5079 at 0.1, 0.2, 0.3, 0.4 and 0.5 levels respectively. This implies that there is a strong relationship between storage and weighted discharge storage at 0.1, 0.2 and 0.3 levels of x (Figures 2a-c), while, the relationship is fair at 0.4 and 0.5 levels (Figures 2d-e).

Table 8. The Summary of the Results

S/N	*x*	K	R^2	NSE	Inflow peak (m^3/s)	Outflow Peak (m^3/s)	Attenuation (m^3/s)	Time Lag (days)
1.	0.1	59.873	0.9999	0.95	0.979	0.3998	0.5792	30
2.	0.2	56.933	0.9451	0.78	0.979	0.4789	0.5001	30
3.	0.3	49.037	0.8091	0.51	0.979	0.6085	0.3705	30
4.	0.4	39.646	0.6502	0.14	0.979	0.7833	0.1957	30
5.	0.5	31.161	0.5079	-0.35	0.979	0.9779	0.0011	30

NB: Nash–Sutcliffe model efficiency coefficient (NSE)

It can be clearly seen from the equations of the plots of storage against weighted discharge storage that the intercepts are negative at levels 0.1 and 0.2 of x while they are positive for levels 0.3, 0.4 and 0.5. The maximum stage of water occurs when the outflow and inflow rates are equal. As inflow reduces, the reservoir will begin to drain and the stage will reduce. When outflow rate is less than the inflow rate, water temporarily stores in the reservoir, this is called storage. The storage was found to be -0.647, -0.2499, 0.8784, 2.2358 and 3.4697 at levels 0.1, 0.2, 0.3, 0.4 and 0.5 of x respectively. This implies that there is variation in the storage at different levels of x. Thus, the storage increases with an increase in level of weighting factor x for the Muskingum routine model.

Figure 3 shows the hydrograph obtained at each level of x. From the hydrograph, attenuation and time lag were obtained. Weighting factor varies inversely proportional to storage time constant (K). It was observed that attenuation is inversely proportional to the weighting factor (x) and directly proportional to storage time constant (K). This implies that the higher the value of weighting factor (x) chosen for calibration the lower the attenuation obtained. Outflow peak is directly proportional to the weighting factor (x) and inversely proportional to storage time constant (K). Inflow peak is constant for every level of weighting factor (x) and storage time constant (K). Time lag is constant at all levels of x and K. This implies that the chosen weighting factor (x) in the calibration does not have influence on the time lag in the prediction, but it has significance effect on attenuation. The results are summarized in Table 8.

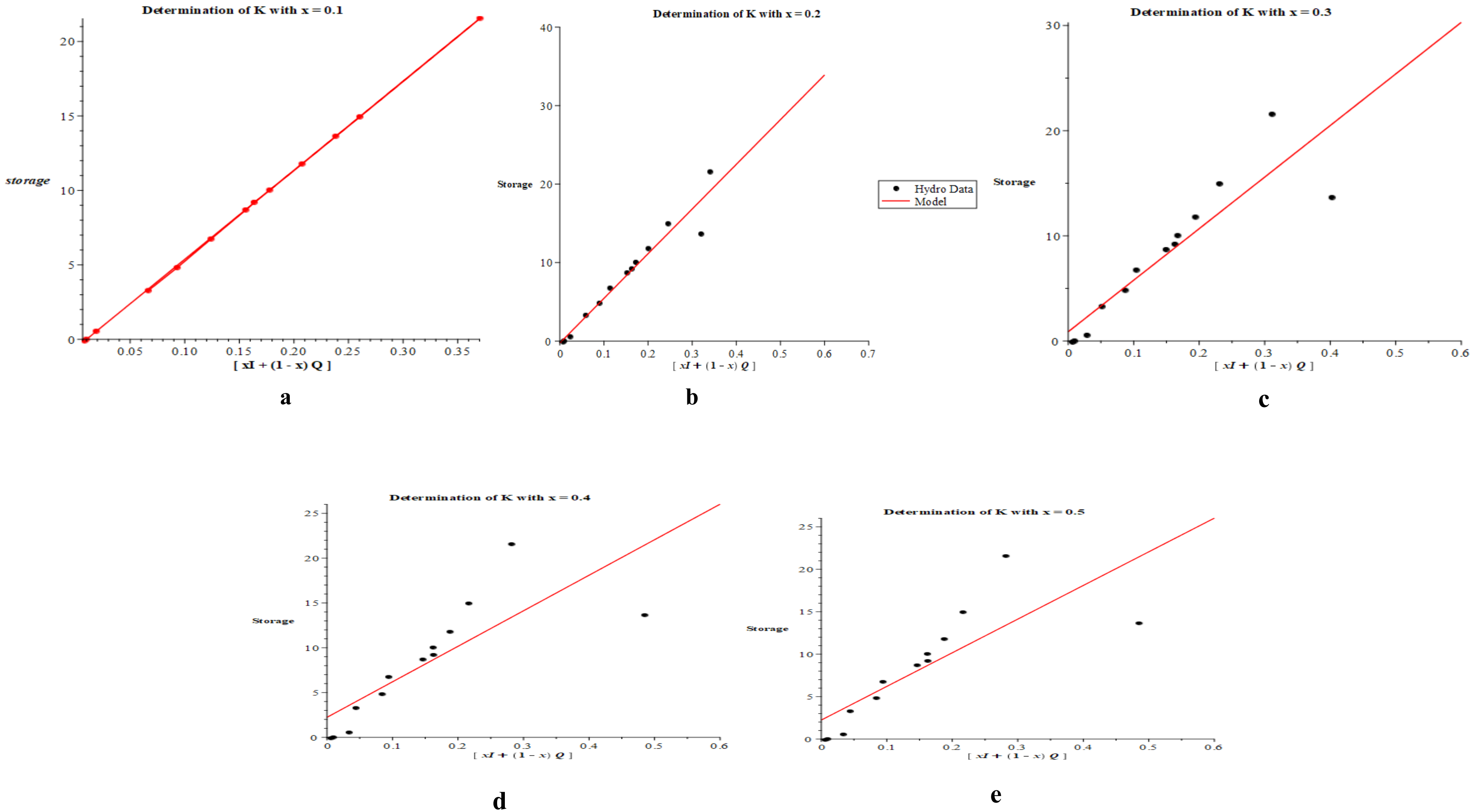

Fig. 2. Plot of Storage (m^3/s.days) against $[xI+(1-x)Q]$ (m^3/s) when *(a)* $x = 0.1$ *(b)* $x = 0.2$ *(c)* $x = 0.3$ *(d)* $x = 0.4$ *(e)* $x = 0.5$

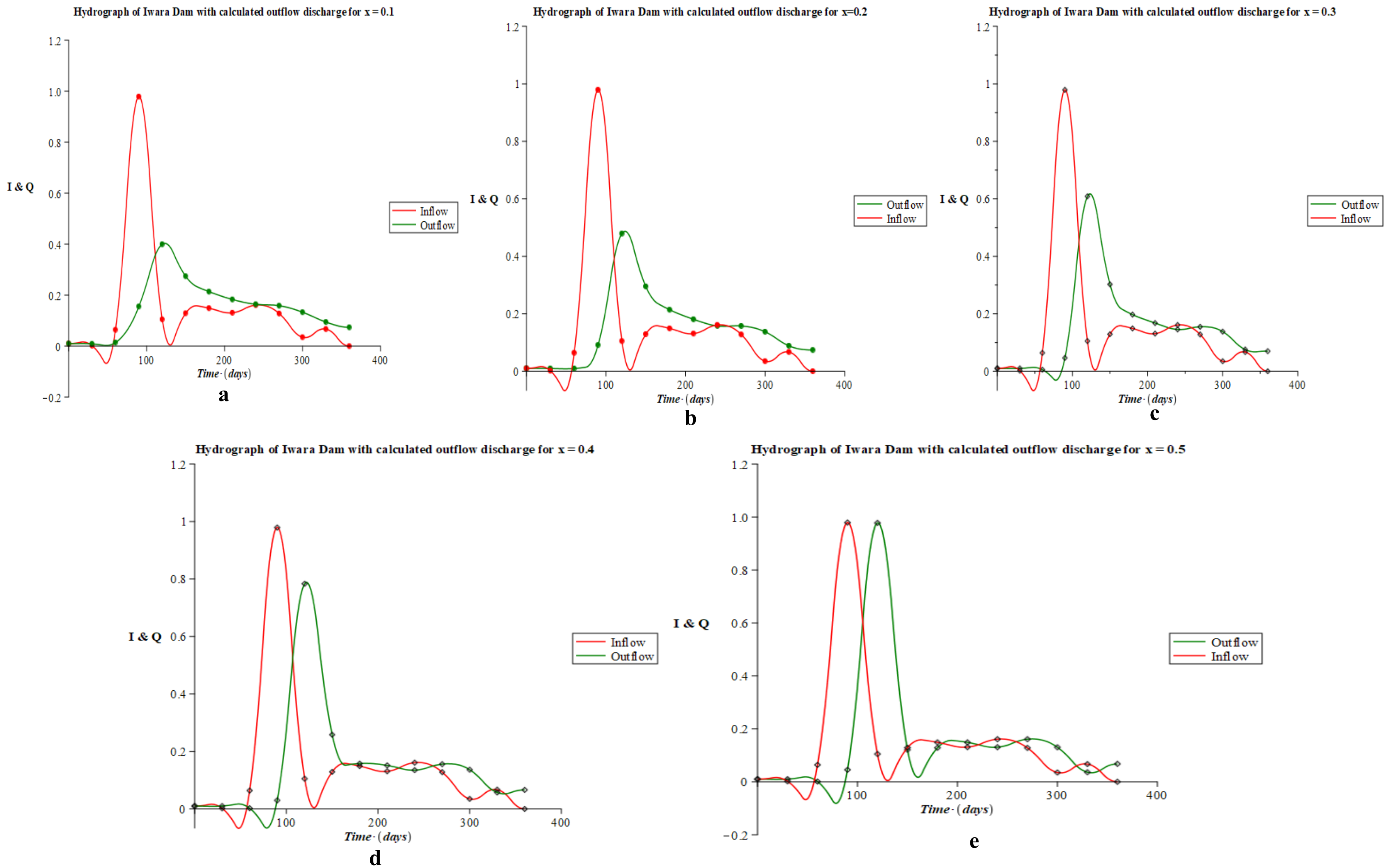

Fig. 3. Plot of Inflow (I) & Outflow (Q) $m^3/s \times 10^6$ against Time (days) when *(a) x=0.1 (b) x=0.2 (c) x=0.3 (d) x=0.4 (e) x=0.5*

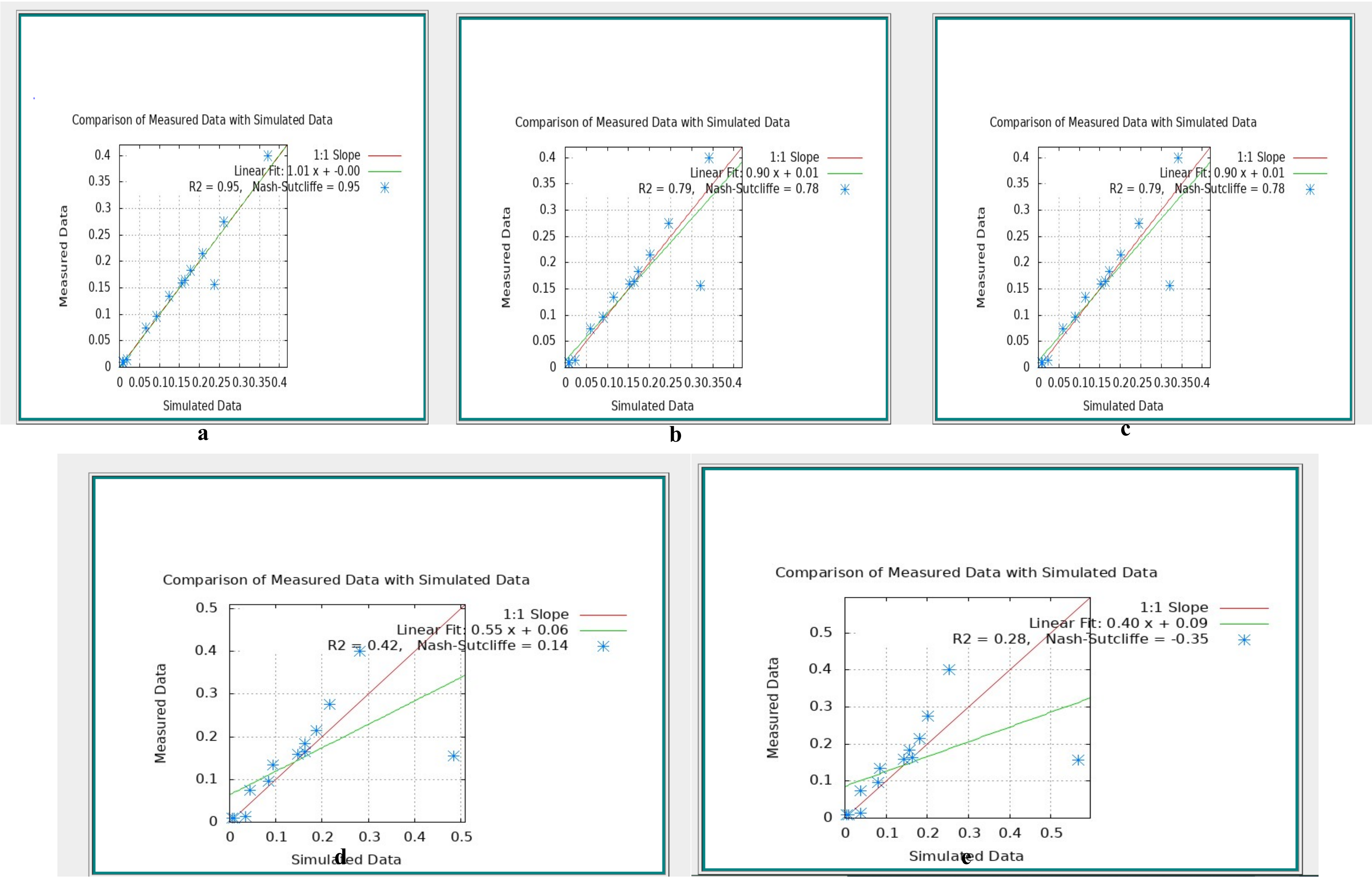

Fig. 4. Plot showing comparison of simulated and measured data for NSE when *(a) x=0.1 (b) x=0.2 (c) x=0.3 (d) x=0.4 (e) x=0.5*

An efficiency less than zero (NSE < 0) occurs when the observed mean is a better predictor than the model data so values of the NSE nearer to 1, suggest a model with more predictive skill. The observed mean for the experimental data is 0.145231. So the values of x=0.1 to 0.3 are more acceptable for the prediction based on the NSE. A test significance for NSE to assess its robustness has been proposed whereby the model can be objectively accepted or rejected based on the probability value of obtaining NSE greater than some subjective threshold (Figure 4).

Nash–Sutcliffe efficiency can be used to quantitatively describe the accuracy of model outputs other than discharge. This indicator can be used to describe the predictive accuracy of other models as long as there is observed data to compare the model results to. For example, Nash–Sutcliffe efficiency has been reported in scientific literature for model simulations of discharge; water quality constituents such as sediment, nitrogen, and phosphorus loading [27]. Other applications are the use of Nash–Sutcliffe coefficients to optimize parameter values of geophysical models, such as models to simulate the coupling between isotope behavior and soil evolution [28].

4. Conclusion

There are essential factors like attenuation, time lag, outflow peak and storage which are required in flood risk prediction and flood pattern. Nevertheless, an accurate prediction strongly depends on appropriate calibration of routine parameters of the flood model, such as weighting factor (x) and storage time constant (K) but the weighting factor being used to determine storage time constant has not been given consideration in past literatures and this could have led to inaccurate prediction in the past.

The Muskingum model was used to obtain the routing parameters and it was observed that all the perform metrics applied decreased with an increased weighting factor (x) which suggests that there is a strong correlation between storage and weighted discharge storage at 0.1-0.3 levels of x while the relationship is fair at 0.4-0.5 levels.

It is therefore appropriate to choose a weighing factor between 0.1 and 0.3 for attenuation prediction, while a weighting factor between 0.4 and 0.5 would be appropriate for accurate prediction of both outflow peak and storage. The weighting factor (x) varies inversely proportional to storage time constant (K), which corroborate with the previous studies. However, the two calibration parameters vary with attenuation and outflow peak. The calibration parameters have a significant effect on both outflow peak and attenuation, which give vital information on the level of risk from flood modeling. Thus, in order to have a good attenuation prediction, a lower value of x will be appropriate. This is so, because x is inversely proportional to the value of K, while x is directly proportional with the outflow peak. This implies that the value of x cannot be chosen arbitrarily because it could lead to inaccurate predictions and this could also lead to over or under prediction in outflow peak.

However, it was observed that the calibration parameter variation does not affect both the inflow peak and time lag of prediction modeling. Based on the research conducted, it is recommended that; in order to have a good attenuation prediction, a level of x ranging from 0.1-0.3 would be appropriate. This is so because as the value of x decreases, the value of attenuation increases. A level of x ranging from 0.4-0.5 would be appropriate for good outflow peak and storage prediction because as the value of x increases, the value of outflow peak and storage increases.

Funding

There is no funding for the research

Conflict of Interest

The authors declare no competing interest

References

[1] Sheshu, E.D., Manjunath, N., Karthik, S., Akash, U., Implementation of Flood Warning System using IoT. In *2018 Second International Conference on Green Computing and Internet of Things (ICGCIoT)*, 445-448. 2018.

[2] Fernandez, D.S., Lutz, M.A., Urban flood hazard zoning in Tucumán Province, Argentina, using GIS and multicriteria decision analysis. *Engineering Geology,* 111, 1-4:90-98, 2010.

[3] Karley, N.K., Flooding and physical planning in urban areas in West Africa: situational analysis of Accra, Ghana. *Theoretical and Empirical Researches in Urban Management*, 4 (13), 25-41, 2009.

[4] Adebayo, W.O., Jegede, A.O., The Environmental Impact of Flooding on Transportation Landuse in Benin City, Nigeria. African Research Review, 390-400, 2010.

[5] Plate, E.J., Flood risk and flood management. *Journal of hydrology,* 267.1-2, 2-11, 2002.

[6] Sivakumar, V.K., Impacts of natural disasters in agriculture, rangeland and forestry: an overview. *Natural disasters and extreme events in Agriculture*, 1-22, 2005.

[7] Wu, H., Adler, R.F., Hong, Y., Tian, Y., Policelli, F., Evaluation of global flood detection using satellite-based rainfall and hydrologic model. *Journal of Hydrometeorology*, *13*(4),1268-1284, 2012.

[8] Freer, J., Beven, K.J., Neal, J., Schumann, G., Hall, J., Bates, P., Flood Risk and Uncertainty. Risk and Uncertainty Assessment for Natural Hazards, Cambridge, UK.190-233, 2011.

[9] Carsell, K.M., Pingel, N.D., Ford, D.T., Quantifying the Benefit of a Flood Warning System. *Natural Hazards Review,* 5(3),131-140, 2004.

[10] Dennis, P., Tunstall, S., Wilson, T., Socio-economic benefits of flood forecasting and warning. *Flood Hazard Research Centre, Middlesex University, Queensway, Enfield, London, UK, 2005.*

[11] Yuan, L., Ryu, D., Western, A.W., Wang, Q.J., Assimilation of stream discharge for flood forecasting: The benefits of accounting for routing time lags. *Water resources research,* 49(4),1887-1900, 2013.

[12] Vieux, B.E., Cui, Z., Gaur, A., Evaluation of a physics-based distributed hydrologic model for flood forecasting. *Journal of hydrology,* 298(1-4), 155-177, 2004.

[13] Mendes, J., Maia, R., Hydrological Modelling Calibration for Operational Flood Forecasting. *Water Resources Management,* 30, 5671-5685, 2016.

[14] Alabi, O.O., Sedara, S.O., Adetoyinbo, A.A., Akinwande, D.D., Estimation of Outflow Discharge from an Ungauged River: Case Study of Awara in Ondo State, Southwestern Nigeria. *FUTA J. of Research in Sci.,* 13(2), 343-349, 2017.

[15] Alabi, O.O., Olawale, S.O., Ogunbiyi, M.A., Sedara, S.O., Akinwande, D.D., Modeling the Flooding of Awara River in Ondo State, Southwestern Nigeria. *Federal University Wukari* (*FUW) Trends in Sci. and Tech. J.,* 2(2):343-349, 2017.

[16] Barati, R., Parameter estimation of nonlinear Muskingum models using Nelder-Mead Simplex algorithm. *J. Hydrologic Eng.,* 16(11), 946-954, 2011.

[17] Govinda, R., Ramana, M.K.V., Application of Muskingum Flood Routing Method for the Dhalegaon-Babli Reach of the Godavari, 512-516, 1989.

[18] Burgan, H.I., Icaga, Y., Flood Analysis Using Adaptive Hydraulics (ADH) Model in the Akarcay Basin, Teknik Dergi, 9029-9051, 2019, https://doi.org/10.18400/tekderg.416067.

[19] Pangali Sharma, T.P., Zhang, J., Khanal, N.R., Nepal, P., Pangali Sharma, B.P., Nanzad, L., Gautam, Y., Household Vulnerability to Flood Disasters among Tharu Community, Western Nepal. Sustainability, 14, 12386, 2022, https://doi.org/10.3390/su141912386.

[20] Mustafa, Y.M., Amin, M.S.M., Lee, T.S., Shariff, A.R.M., Evaluation of land development impact on a tropical watershed hydrology using remote sensing and GIS. *Journal of spatial hydrology*, *5*(2), 2012.

[21] Zoppou, C., Reverse routing of flood hydrographs using level pool routing. *J. Hydrologic Eng., 4*(2),184-188, 1999.

[22] Ramírez, J.A., Prediction and modeling of flood hydrology and hydraulics. *Inland flood hazards: Human, riparian and aquatic communities*, 498, 2000.

[23] Chow, V.T., Maidment, D.R., Mays, L.W., Applied Hydrology. McGraw-Hill International Editions: Singapore, 1988.

[24] McCarthy, G.T., The unit hydrograph and flood routing, Conference of the North Atlantic Division, U.S. Army Corps of Engineers, 1938.

[25] Song, X., Kong, F., Zhao-Xia, Z.H.U., Application of Muskingum routing method with variable parameters in ungauged basin. *Water Sci. Eng.,* 2011.

[26] UNIDO-RC-SHP, Detailed project report for Awara dam/Oyibo River Small Hydro Power Development, Ikare-Akoko, North East LGA Ondo State by UNIDO Regional Center for Small Hydro Power in Africa, Abuja, Nigeria, 2010.

[27] Moriasi, D. N., Arnold, J.G., Van Liew, M.W., Bingner, R. L., Harmel, R.D., Veith, T.L., Model Evaluation Guidelines for Systematic Quantification of Accuracy in Watershed Simulations. Transactions of the ASABE, 50(3), 885–900, 2007, doi:10.13031/2013.23153.

[28] Campforts, B., Vanacker, V., Vanderborght, J., Baken, S., Smolders, E., Govers, G., Simulating the mobility of meteoric 10 Be in the landscape through a coupled soil-hillslope model (Be2D). Earth and Planetary Science Letters. 439: 143–157, 2016.